IEEE Access
Multidisciplinary | Rapid Review | Open Access Journal

Received 31 December 2022, accepted 18 January 2023, date of publication 23 January 2023, date of current version 6 February 2023.

Digital Object Identifier 10.1109/ACCESS.2023.3238870

RESEARCH ARTICLE

A Unidirectional Cascaded High-Power Wind Converter With Reduced Number of Active Devices

YONGLEI ZHANG, (Member, IEEE), XIN PENG, XIBO YUAN, (Senior Member, IEEE), YAN LI, AND KAI WANG

School of Electrical Engineering, China University of Mining and Technology, Xuzhou 221116, China

Corresponding author: Xibo Yuan (yuanxibo@ieee.org)

This work was supported by the Fundamental Research Funds for the Central Universities under Grant 2019QNA15.

ABSTRACT For large offshore wind turbines, cascaded H-bridge wind power converters can raise the wind generator voltage to a medium voltage level such as 10kV, which is favored for reducing the generator current, mitigating issues such as cable twisting in low-voltage, high-current configurations. In order to reduce the number of required active power devices, this paper presents a unidirectional-power-flow medium voltage high-power cascaded wind power converter. The proposed topology uses a unidirectional cascaded H-bridge rectifier as the generator-side converter to connect the medium-voltage permanent synchronous wind generator. The proposed topology reduces the number of active power devices and their associated gate driver circuits, control, etc. A zero deadtime modulation method is also presented for the generator side converter, which can eliminate the deadtime and improve the voltage and current waveform quality. Furthermore, the proposed topology will not increase the converter power losses as analyzed in the paper, or sacrifice dynamic control performance. Simulation and experiment results are presented, which validate the proposed unidirectional power conversion system.

INDEX TERMS Cascaded H-bridge, unidirectional power flow, wind power converter, zero deadtime modulation.

I. INTRODUCTION

Wind power as a renewable energy source plays an important role in low-carbon, clean and sustainable energy systems [1]. In the past two decades, wind power has experienced rapid development and the cumulative global installed wind power capacity has reached 837GW in 2021 [2] and is still growing rapidly.

The increase of wind power installation also promotes the development of wind power converter technologies [3], [4], [5], [6], [7]. Wind power converters are critical equipment in wind power conversion systems, transferring power from the wind generator to the grid [3]. The mainstream high-power (MWs) variable-speed wind converter technologies are based on either doubly-fed-induction-generators (DFIGs) with partially rated rotor-side converters [7] or direct-drive permanent magnet synchronous generators (PMSGs) with full-power back-to-back converters [8]. Conventionally, the voltage level for these systems is 690V.

In order to increase the amount of captured wind power per turbine and reduce the average cost of wind power generation, the power level of a single wind turbine also increases rapidly [9]. In addition, it is generally the case that the maintenance cost of fewer larger wind turbines is lower than those with smaller wind turbines. Hence, larger wind turbines are preferred. At present, the power rating of a single offshore wind turbine has reached 14MW, and is being developed towards even higher power levels [10]. For large wind turbines in the range between 10-20MWs, the low-voltage (e.g., 690V) systems suffer from many engineering issues, such as excessive current, large number of paralleled units, lower efficiency, and difficulty in twisting bulky cables [11].

The associate editor coordinating the review of this manuscript and approving it for publication was R. K. Saket.

Development of medium-voltage high-power wind converters is an effective way to mitigate the above issues. In the medium voltage range (3kV∼33kV), the neutral-point clamped (NPC) three-level wind power converters are widely used where the converter AC side voltage can cover 1.14kV, 3.3kV or 4.16kV [5], [12], [13], [14]. One of the concerns of multilevel converters is the large number of active power devices needed. In view of the unidirectional power flow characteristics of wind turbines, i.e., from the generator to the grid, in order to reduce the number of power devices, the unidirectional Vienna-type three-level converter can be used, where the main active power devices such as IGBTs can be replaced by diodes [15], [16], [17]. This simplification thanks to the unidirectional power flow can reduce the cost of power devices, reduce the number of required gate drivers, reduce failure rates of the active devices and remove the need of deadtime in the modulation. However, the above NPC-type converters still suffer from reliability issues, where when one of the devices of the converter fails, the whole converter has to stop running. This can be problematic given the high maintenance and repair cost/cycle for offshore applications. Furthermore, with the three-level structure, the AC-side voltage cannot exceed 4.16kV without connecting devices in series. Hence, paralleling converters or devices are still needed due to the high current in high-power wind turbines

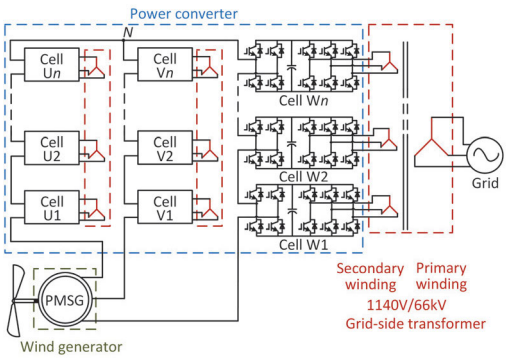

FIGURE 1. Wind power conversion system using the cascaded H-bridge converter.

In order to further raise the voltage level, a cascaded H-bridge (CHB) wind power converter topology was presented in [11], [19], as shown in Fig.1. This topology has a similar structure as the conventional CHB converter in motor drive systems, but with the opposite power flow direction. The wind generator is connected to the CHB rectifier where the generator voltage can be as high as 10kV, and each H-bridge unit is connected to the grid (33kV or 66kV) through a three-phase inverter and a multi-winding grid-frequency (50Hz/60Hz) transformer. The higher voltage level can be achieved by this topology using low-voltage power devices. The high voltage, hence the lower current can significantly reduce the copper losses (I^2R), cable weight and mitigate the cable twisting problem. Moreover, it has a modular structure and fault-tolerant operation capability, which is suitable for 10-20MW large wind turbines.

However, in this topology shown in Fig. 1, each CHB converter is in essence a single-phase converter, where there is large low-frequency (double of the fundamental frequency) power ripple in each cell, requiring large DC capacitors to attenuate the dc-link voltage ripple. In [19], a control method was proposed to balance the power, including the ripple power, between the grid-side inverter and the H-bridge rectifier, thus reducing the required dc-link capacitors. Reference [20] further proposes a new cascaded wind power converter based on a four-port isolated DC/DC converter as shown in Fig. 2, to eliminate the low-frequency pulsating power. In this topology, the low-frequency power ripple from the single phases can be transferred to the magnetic core of the four-winding high-frequency transformers and then cancelled.

Although the cascaded H-bridge wind power converter shows many advantages as mentioned above, a large number of power devices are required. In [22], several unidirectional-power-flow rectifiers are evaluated and compared, proving the unidirectional-power-flow cascaded H-bridge rectifier has lower cost and higher reliability. In [23], the modeling and control of unidirectional power-flow cascaded H-bridge rectifier was presented. Conventional unidirectional power flowing converter has to work at unity power factor condition. Otherwise, the converter current will be distorted at the zero-crossing points. In contrast, the unidirectional-power-flow cascaded H-bridge rectifier has the ability to work when the power factor is lower than 1, as analyzed in [24].

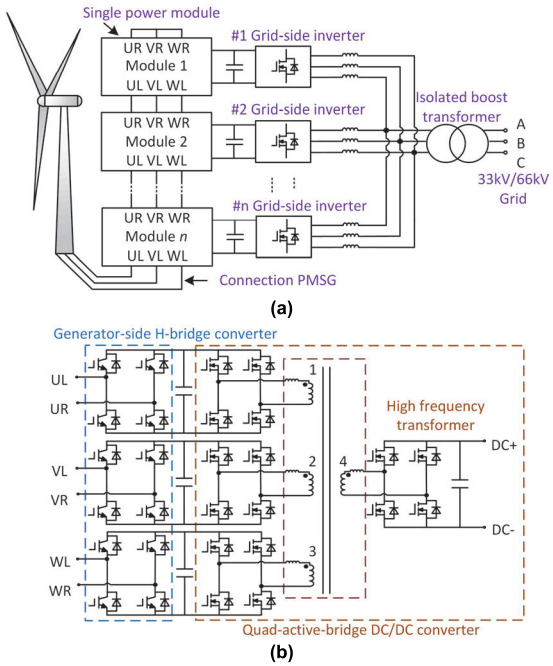

FIGURE 2. Power conversion system using the cascaded H-bridge converter with quad-active-bridge DC/DC converter in wind power systems [20]: (a) The overall structure and (b) single power module.

Based on the topology in Fig. 2, this paper presents a unidirectional-power-flow medium-voltage cascaded wind power system by replacing two active power devices with diodes at the upper bridge arm in each H-bridge rectifier as will be shown in Fig.3 and Fig.4. Reducing the number of power devices is beneficial for reducing the cost of power devices and improving the system reliability. The proposed topology can realize wind power generation in steady-state and dynamic conditions without increasing the system losses or sacrificing control performance. Moreover, with a proposed zero deadtime modulation method, there is no need to set deadtime for the generator-side converter, which is beneficial for reducing the low-frequency harmonics of the converter output voltages and currents. Finally, simulation and experiment results are presented, which verifies the presented system.

II. UNDIRCTIONAL-POWER-FLOW WIND POWER CONVERTER

For each H-bridge cell, after replacing the two power devices in the upper bridges with two diodes, unidirectional-power-flow H-bridge cell can be derived as shown in Fig. 3. In this case, the power can only flow from the AC side to the DC side. Fig. 4 shows the topology of a single power module, where the input rectifiers have all been replaced with the unidirectional structure (two diodes) in comparison to the original structure shown in Fig.2(b). The overall configuration of the wind converter is the same as that shown in Fig. 2(a), where only the input rectifiers are changed. The proposed topology not only can reduce the number of required active power devices of the generator-side converter (rectifier) by half, but also can output the same high voltage as the original converter shown in Fig.2. Therefore, for a 10kV/15MW offshore wind power system, the number of required power devices can be significantly reduced given the large number of cells used.

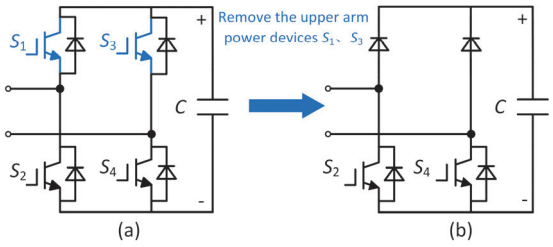

FIGURE 3. Derivation of unidirectional-power-flow H-bridge converter (rectifier): (a) H-bridge cell and (b) unidirectional H-bridge cell.

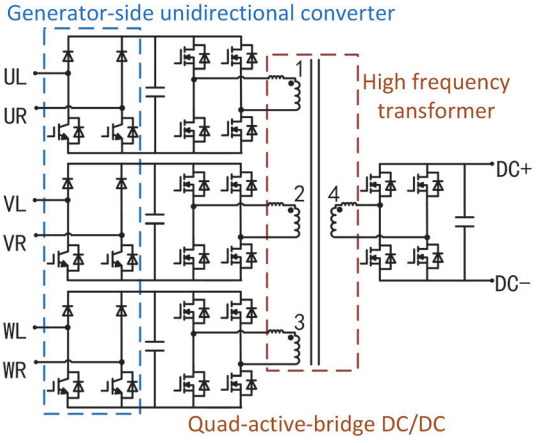

FIGURE 4. One power module of the proposed the wind power generation system with unidirectional-power-flowing.

Assuming low-voltage (e.g. 1700V) power devices are selected to construct the proposed converter, the dc-link voltage of the cascaded H-bridge converter can be set around 1100V. Then, the number of cascaded stages n will be

$$n \geq \frac{u_g}{\sqrt{3} \times \frac{u_{dc}}{\sqrt{2}}} = 8.16 \approx 9. \tag{1}$$

For a 15MW/10kV wind turbine system, the rated current of the generator-side converter can be calculated by

$$i_g = \frac{P}{\sqrt{3} u_g} = 866A. \tag{2}$$

As seen, since the cascaded H-bridge converter can raise the generator voltage level to 10kV, the corresponding current is not very large (866A) for a 15MW wind turbine. At present, the current rating of a single 1700V IGBT device can reach 3600A and that of a single 1700V fast diode can reach 1800A. Therefore, the proposed generator-side CHB converter (rectifier) with unidirectional power flow for a10kV/15MW wind turbine system can be built with commercially available power devices. For example, with some margin, the active power devices can use the 1700V/1600A IGBT module FZ1600R17HP4_B21 from Infineon and the diodes can be 1700V/1800A fast diode module RM1800HE-34S from Mitsubishi. Basically, diodes with a similar current rating as the IGBTs can be used. For the isolated DC-DC converters shown in Fig.4, if IGBT devices are used, the current level of a single commercial IGBT is sufficient to output the required power. However, if SiC MOSFETs are used to construct the above system, the current level of a single commercial SiC MOSFET may not be enough at present, given the required safety margin. Hence, two or three SiC MOSFETs can be connected in parallel to output the required power, e.g, using 1700V/650A SiC MOSFETs from Wolfspeed.

III. ZERO DEADTIME MODULATION METHOD

One important advantage for the proposed converter is that deadtime is not required for the generator-side converter. This section presents a zero deadtime modulation method to control the generator-side converter.

For the conventional cascaded H-bridge converter, a deadtime is required to avoid short circuit state between the upper and lower switches. However, the existence of deadtime will

negatively affect the converter output voltage, introducing low-frequency harmonics. In general, the negative effect of deadtime varies with the modulation index M. With the decrease of the modulation index, the negative effect of the deadtime will be more obvious. For the wind power system, below the rated wind speed, the wind generator speed need to track the change of wind speed and thus output more power (maximum power point tracking, MPPT). Therefore, the modulation index of the generator-side converter can be low, where generator stator voltage and current can contain low-frequency harmonics, which increases the losses of generator, raise the temperature of windings and cause torque fluctuation issues.

A. ZERO DEADTIME MODULATION METHOD

Since the power devices of the upper bridge has been replaced by diodes in the proposed converter, the upper bridge and lower bridge will not be conducting at the same time (shoot through). Therefore, there is no need to set the deadtime. However, given the unidirectional-power-flow cascaded H-bridge cannot output negative voltage level, extra modulation techniques should be used to ensure the proper operation of the converter.

Fig. 5 shows six effective working states of a unidirectional-power-flow H-bridge converter. Here, the positive direction of the current i_x is flowing from the AC side to the DC side. When i_x is positive, if the reference voltage u_x is also positive, the converter can output positive voltage or zero voltage as shown in Fig. 5(a) and Fig. 5(b), respectively.

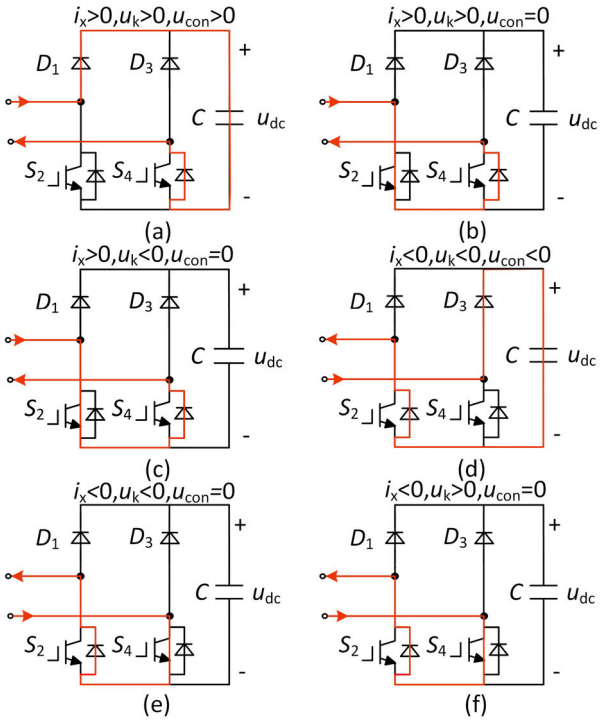

FIGURE 5. Six working states of one unidirectional power flow cell.

If the reference voltage u_x is negative, the converter can only output zero voltage as shown in Fig. 5(c). When i_x is negative, there are three other switching states as shown in Fig. 5(d) to Fig. 5(f).

Based on the above analysis, a zero deadtime modulation method can be derived for the proposed unidirectional-power flow converter, where the flowchart is shown in Fig. 6. As can be seen, this method is like the phase disposition modulation method, but the direction of current i_x should be judged. Specifically, when the current direction is positive, the converter does not have the ability to output negative voltage. In this case, if the reference voltage is negative, the converter will output zero voltage level. While if the reference voltage is positive, the converter can directly output the desired voltage level. When the current direction is negative, the converter does not have the ability to output positive voltage, meaning the positive reference voltage should be replaced by the zero-voltage level.

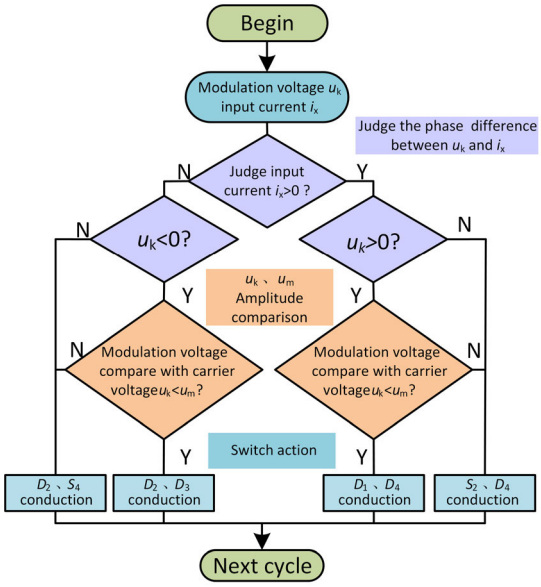

FIGURE 6. Flowchart of the zero deadtime modulation method.

B. LOSSES ANALYSIS

This part analyzes the power losses of the generator-side converter. The power losses of the power device consist of two parts, i.e., the conduction loss $P_{\mathrm{con,X}}$ and the switching losses $P_{\mathrm{sw,X}}$ [25], as presented in (3) and (4), as shown at the bottom of the next page, where, $f(\omega t)$ is the modulation function, representing the device conducting duty cycle, which varies for different devices; v_{ce0} is the device initial voltage drop; i_{cm} is the load peak current; r_0 is the equivalent resistance, representing the linear region of the device voltage drop; f_{sw} is the switching frequency; v_{ce} is the device voltage drop; v_{ceN} is the device voltage drop at the rated current. A_0, B_0, C_0 describes the relationship between the switching energy and current.

In order to compare the power losses of the conventional phase disposition modulation for the CHB converter and the proposed zero dead-time modulation for the proposed unidirectional power flow CHB converter. Fig. 7 shows the conducted power devices within one fundamental generator output cycle of the above two modulation methods. Table 1 lists the conduction intervals and modulation function for the phase disposition modulation and the proposed zero dead-time modulation method. Table 2 lists the switching intervals of the two methods. As seen, when the polarity of the converter voltage and current are the same, the conducted power devices of the two modulation methods are the same. When the converter voltage and current are opposite, the conducted power devices are different. Further, considering the generator-side converter is usually working around unity power factor ($\cos\theta = 1$), the polarity of the converter voltage and current will be the same in most of the time, meaning the power losses of the two methods can be treated as the same.

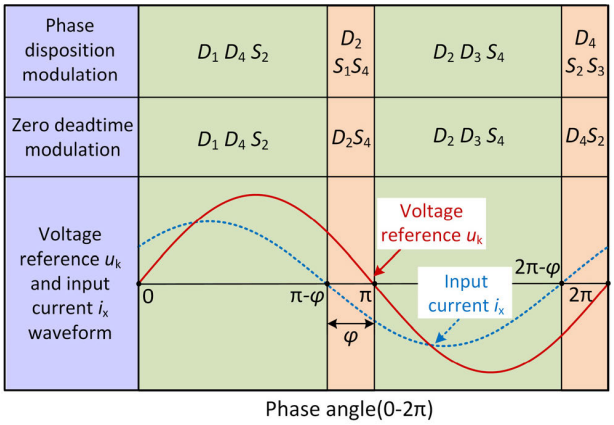

FIGURE 7. The conducted power devices of two kinds of converters within one generator cycle.

TABLE 1. The conduction interval and modulation function.

Switch	D_1	S_1	S_2		D_2	
Phase disposition conduction interval	$[0,\pi-\varphi]$	$[\pi-\varphi,\pi]$	$[0,\pi-\varphi]$	$[2\pi-\varphi,2\pi]$	$[\pi-\varphi,\pi]$	$[\pi,2\pi-\varphi]$
Zero deadtime conduction interval	$[0,\pi-\varphi]$	/	$[0,\pi-\varphi]$	$[2\pi-\varphi,2\pi]$	$[\pi-\varphi,\pi]$	$[\pi,2\pi-\varphi]$
Phase disposition $f(\omega t)$	$M\sin(\omega t)$	$M\sin(\omega t)$	$1-M\sin(\omega t)$	1	$1-M\sin(\omega t)$	1
Zero deadtime $f(\omega t)$	$M\sin(\omega t)$	/	$1-M\sin(\omega t)$	1	1	1

In order to verify the above analysis, the simulation model of a 10kV/15MW cascaded H-bridge wind power system with five stages is built in PLECS. The power devices are

TABLE 2. The switching intervals of the two modulation methods.

The Switching Interval	D_1	S_1	S_2	D_2
Phase disposition switching interval	$[0,\pi-\varphi]$	$[\pi-\varphi,\pi]$	$[0,\pi-\varphi]$	$[\pi-\varphi,\pi]$
Zero deadtime switching interval	$[0,\pi-\varphi]$	/	$[0,\pi-\varphi]$	/

TABLE 3. The device loss and converter efficiency of the two converters under different modulation methods.

Modulation method	Carrier frequency f_c(Hz)	Equivalent switching frequency(Hz)	Device loss(kW)	Converter efficiency
Carrier phase shifted	2k	20k	404	97.31%
Phase disposition	20k	20k	392	97.39%
Zero deadtime	20k	20k	384	97.44%

the 3300V/1500A IGBT power modules (FZ1500R33HL3) from Infineon. Table 3 shows simulated power losses for the cascaded H-bridge converter and the proposed unidirectional power-flow converter. For the conventional converter, the phase-shifted or phase disposition modulation can be used. The zero dead time modulation method is used for the proposed unidirectional power-flow wind power converter. As seen, when the equivalent switching frequencies of the three methods are configured as 20kHz, the practical switching frequency of each power device will be 2kHz. Therefore, the power losses of these methods are almost the same.

These simulation results for power losses can prove the proposed modulation method will not introduce extra losses with reduced number of active power devices.

Fig. 8 shows the simulated power losses for the CHB converter and the proposed wind power converter. As seen, the proposed unidirectional-power-flow power converter have similar conduction losses and switching losses with the conventional CHB converter when the equivalent switching frequencies are the same.

IV. ANALYSIS OF THE CURRENT DISTORATION ISSUES FOR WIND POWER SYSTEMS

In general, unidirectional-power-flow converters, e.g. the classical Vienna converter, should work at the unity power factor condition. Otherwise the converter current will be distorted at zero-crossing points. In contrast, the proposed unidirectional-power-flow converter can still work well when

$$p_{con,x} = \frac{1}{2\pi}\int_{\theta_1}^{\theta_2} f(\omega t)\times\{v_{ce0}\times i_{cm}\sin(\omega t+\varphi)+r_0\times(i_{cm}\sin(wt+\varphi))^2\}d\omega t \tag{3}$$

$$p_{sw,x} = \frac{f_{sw}}{2\pi}\times\frac{v_{ce}}{v_{ceN}}\int_{\theta_1}^{\theta_2}\{A_0+B_0\times i_{cm}\sin(\omega t+\varphi)+C_0\times(i_{cm}\sin(wt+\varphi))^2\}d\omega t \tag{4}$$

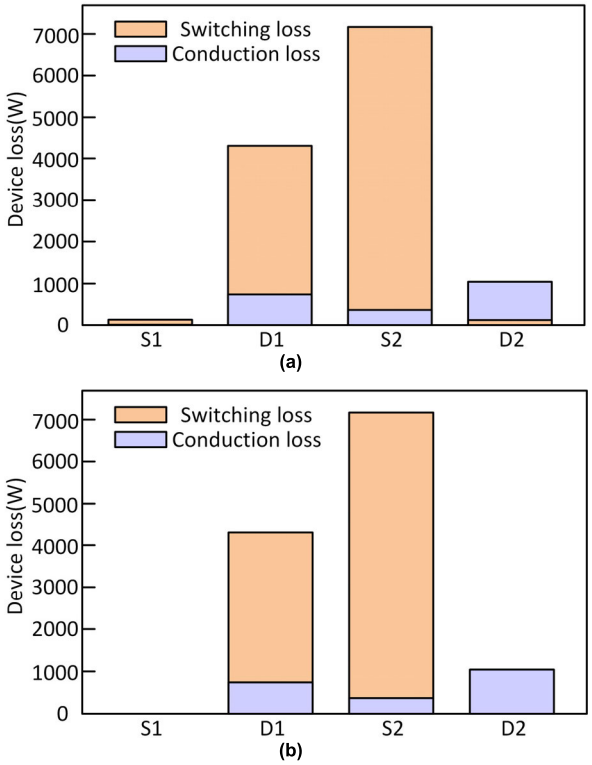

FIGURE 8. Device power losses of two converters: (a) H-bridge cell using phase disposition modulation and (b) unidirectional-power-flow converters using zero deadtime modulation.

the power factor is not 1, depending on the modulation index M.

Fig. 9 shows the current distortion areas for different modulation indexes M and power factors. The shaded area represents the current distortion area. As seen, in the high modulation index region, the converter should work around the unity power factor to avoid current distortion. Whereas, in the low modulation index region, the converter can still work well with current distortion when the power factor is not unity. Therefore, the proposed wind power system can work well in the low modulation index region under non-unity power factor cases.

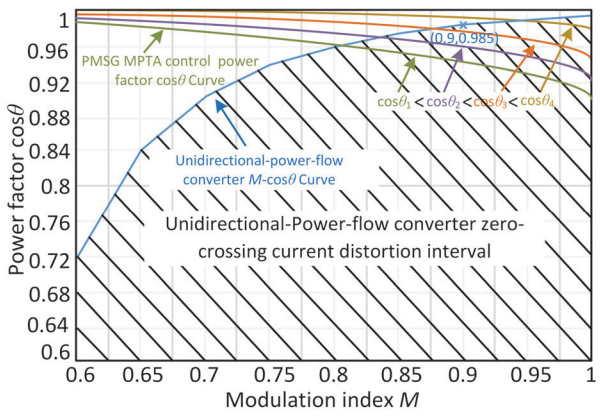

FIGURE 9. The unidirectional-power-flow system PMSG MPTA control zero-crossing current distortion.

Generally, there are two kinds of control methods that can be used to control the PSMG. The first kind of method is the unity power factor control (UPF) method, as shown in Fig. 10. The reactive power current reference is configured as zero to ensure generator output voltage and the current are controlled under unity power factor condition. This method can improve the generator power factor and reduce power losses of the generator-side converter. There is no doubt that the UPF control method can be directly adopted for controlling the proposed wind power converter with the unidirectional power flow structure.

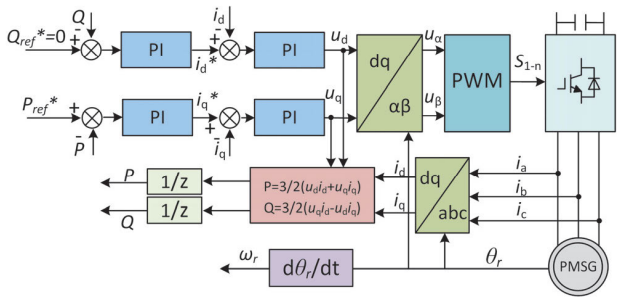

FIGURE 10. The unity power factor control diagram for PMSG.

The other method is the maximum torque per ampere (MPTA) control [26], where the stator current is controlled to be minimal for producing the same electromagnetic torque. This method has more superior dynamic performance to track the wind power fluctuation and thus regulate the wind turbine speed quickly in a wide range. The corresponding power factor of this control method is related to the modulation index M, as plotted in Fig. 9. Specifically, with the increase of the modulation index, the corresponding power factor will be reduced. Then, there are possible overlaps between the MPTA control and the current distortion region of the proposed converter. Whether the generator current will be distorted will be determined by the power factor of the PSMG.

Generally, the power factor is relatively high for high-power PMSGs. In this case, the proposed converter can work well if using the MPTA control method. For the PMSG with a lower power factor, the generator current may be distorted at the rated condition. In this case, the MTPA control and the UPF control method can be combined to control the proposed converter, where the MPTA control is used in the low modulation index range and the UPF control is used in the high modulation index range.

V. SIMULATION AND EXPERIMENT RESULTS

A. SIMULATION RESULTS

In order to validate the feasibility of the proposed unidirectional-power-flow wind power system, a 10kV/15MW medium voltage high power wind power simulation system has been built in MATLAB/Simulink. The generator converter consists of 5 stages (15 cells) and the DC-link voltage

TABLE 4. PMSG rated parameters.

Parameters	values
D、Q axis inductance	0.008H
Stator pole pairs	90
Generator rated frequency	15Hz
Rated voltage	10kV
Rated current	866A
Rated power	15MW

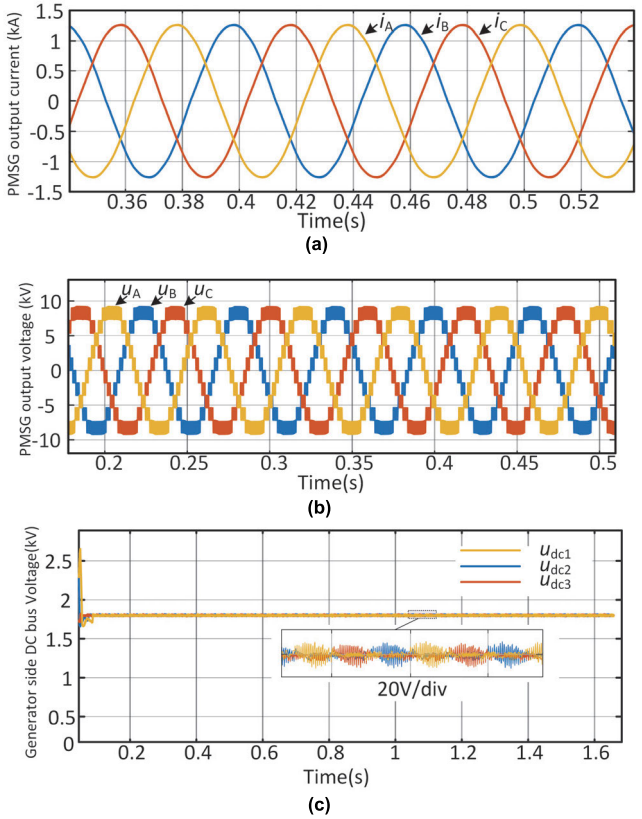

FIGURE 11. Unidirectional-power-flow wind power system generator side converter outputs at the rated condition: (a) PMSG output current; (b) PMSG output voltage and (c) the generator-side converter DC-bus voltage.

of each cell is 1800 V. Table 4 shows the parameters of the PMSG.

Fig. 11 shows the output current, output voltage and DC-bus voltage of the generator-side converter at the rated condition ($M = 0.9$). As seen, the generator-side converter can operate well, where the three-phase currents can be regulated well and there is no current distortion at the zero-crossing instants. In addition, the generator-side converter output phase voltages have 11 voltage levels. The DC-link voltages can be controlled well with very small voltage ripples, as shown in the zoomed waveforms in Fig.11(c).

Fig. 12 shows the dynamic simulation results using the MTPA control method. At 0.3 s, the PMSG power is reduced from 5MW to 3MW. At 0.7s, the PMSG power is increased from 3MW to 15MW. As seen, the generator-side converter can quickly regulate the generator torques and currents.

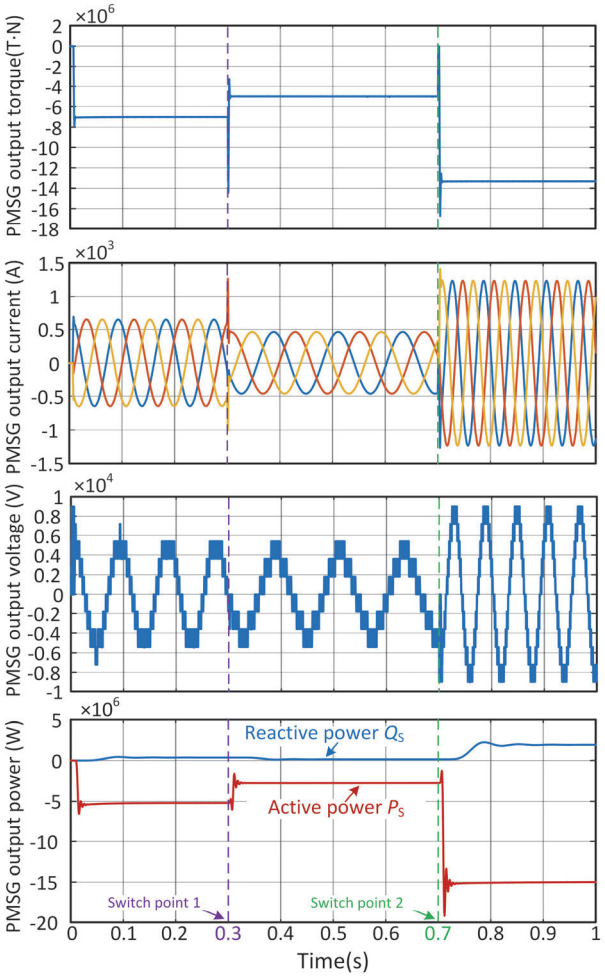

FIGURE 12. Simulation results for the generator-side converter at the dynamic state.

Above simulation results show that the proposed system can work well for the steady and dynamic states. Fig. 13 shows the measured total harmonic distortion (THD) values of the generator-side converter output current for the three modulation methods (carrier phase shifted, phase disposition, zero deadtime modulation) under various modulation indexes. As seen, with the increase of the modulation index, both the current THD of the three methods can be reduced. Moreover, the proposed zero dead time modulation method has more superior performances than the other two modulation methods, especially when the converter is working at the low modulation index range.

B. EXPERIMENT RESULTS

In order to verify the practical performance of the proposed unidirectional-power-flow wind power system, a down-scaled experimental prototype has been built, as shown in Fig. 14. The number of cascaded stages is one. Both the generator-side converter and the grid-side converter are built by the 1200V/50A IGBT intelligent power module (PM50RL1A120) from Mitsubishi Corporation.

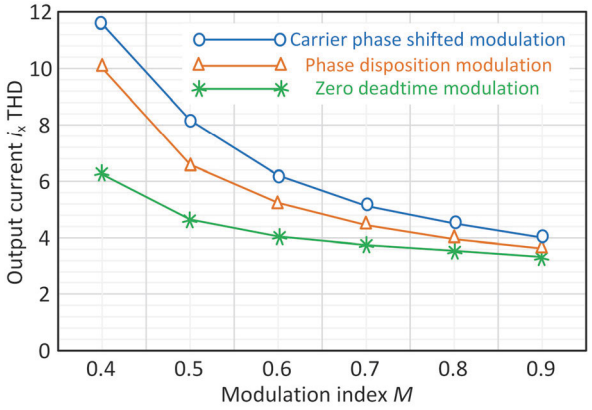

FIGURE 13. Comparison of the current THD for different modulation methods under various modulation indexes.

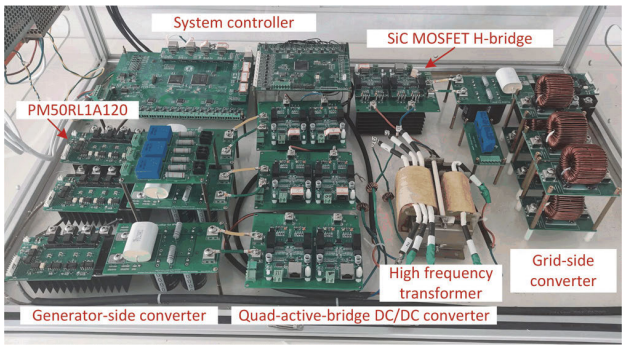

FIGURE 14. Experimental prototype.

TABLE 5. Experimental parameters.

Parameters	values
Rated power	2kW
Input voltage frequency	50Hz
Input side filter inductance	4mH
DC/DC switching frequency	50kHz
Transformer leakage inductance	100uH
DC side voltage	300V

The power devices of the isolated four-port DC/DC converter are the 1200V/30A SiC MOSFETs from Wolfspeed (C2M0080120D), where the switching frequency is 50kHz. Detailed experimental parameters are given in Table 5.

Fig. 15 shows the steady state waveforms of the generator-side current. It can be seen that the output currents of the generator-side converter are symmetrical and sinusoidal. There is no current distortion at the zero-crossing instants. Fig. 16 shows the waveform of the converter output voltage and DC-link voltage at the generate side. As seen, the whole system can work well at the rated operating point.

Fig.17 shows the experimental results at the dynamic state. It can be seen that the system can quickly respond to the change of input power. The above results can prove that the proposed topology has good dynamic performance and can realize stable operation under power fluctuation conditions.

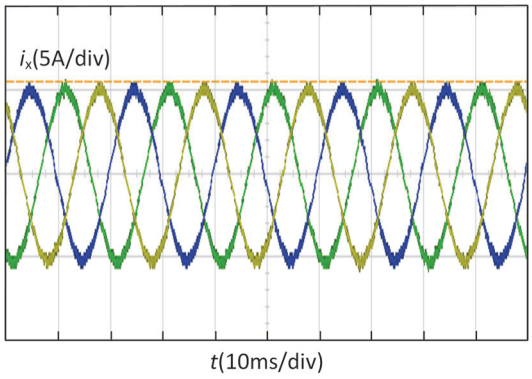

FIGURE 15. Experimental waveforms of the generator-side converter current at the steady state.

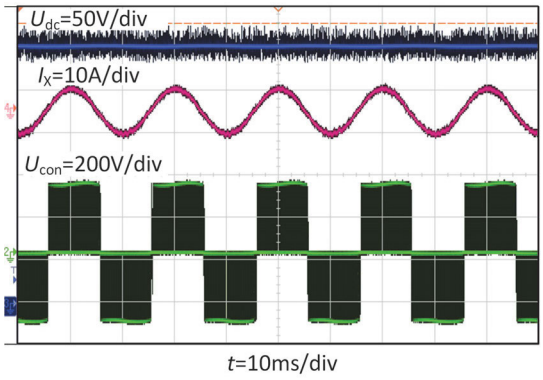

FIGURE 16. Experimental results of the Phase-C input voltage, input current and the DC-link voltage of the generator-side converter.

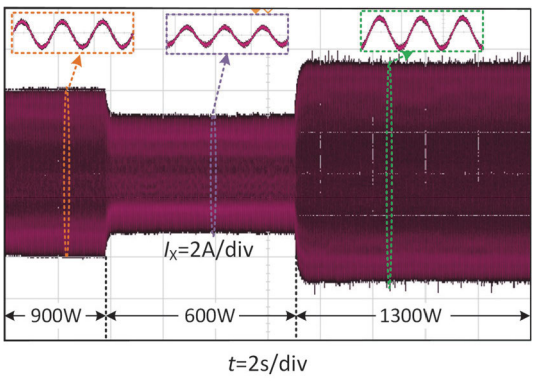

FIGURE 17. Experimental waveforms of Phase-C current at the dynamic state.

Fig. 18 shows the comparison of the frequency spectrum of the converter output voltage for two kinds of converters, i.e., the conventional CHB converter and the proposed unidirectional CHB converter. For the conventional CHB converter, phase disposition modulation is used and the dead time is 2.2 μs. And the zero dead time modulation is used for the proposed converter. The modulation is 0.7 in Fig. 18(a) and the modulation is 0.9 in Fig.18(b). These results can prove

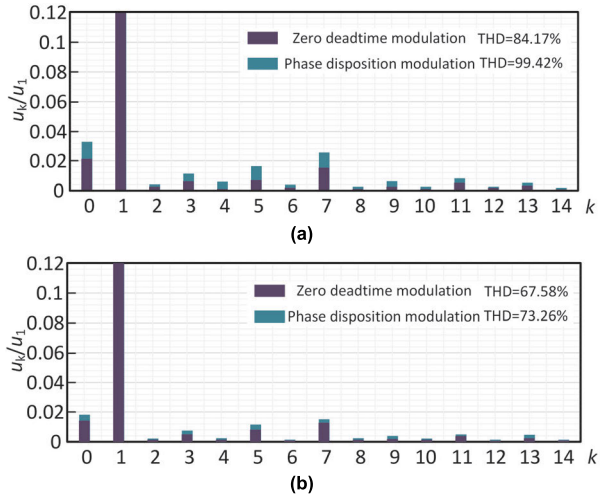

FIGURE 18. Low-frequency harmonics (k<=14) contents of input voltage of two kinds of generator side converter: (a) Modulation index M=0.7 and (b) modulation index M=0.9.

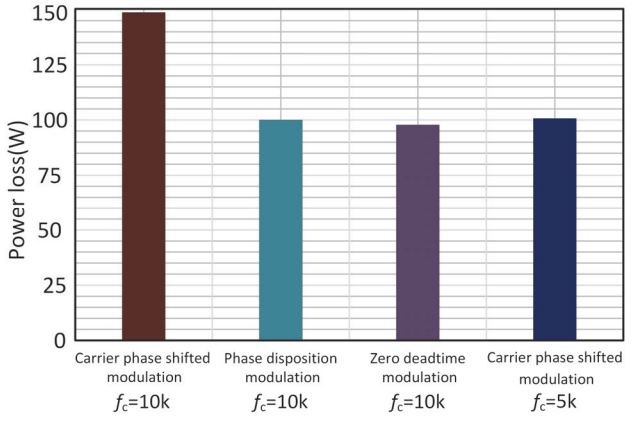

FIGURE 19. Measured power losses of generator-side converter using different modulation methods.

the proposed modulation method have much better current quality, especially when the modulation index is low.

Fig. 19 shows the measured power losses of the generator-side converter, by a power analyzer (WT1800 from YOKOGA). As seen, the power losses of the zero deadtime modulation and the phase disposition modulation are basically the same, where the carrier frequency is 10kHz. For the carrier phase shifted modulation method, the equivalent switching frequency is twice of the switching frequency of the power devices. When the carrier frequency for this modulation method is configured as 10kHz, the corresponding equivalent switching frequency will be 20kHz, where the power losses will be larger than other two methods. If reducing the carrier switching frequency to 5kHz, the equivalent switching frequency switching frequency will be 10kHz and the power losses will be the same as the other two methods. These results can prove the proposed topology will not increase the power losses compared to the standard CHB wind power system.

VI. CONCLUSION

In this paper, a unidirectional-power-flow medium voltage high power cascaded wind power converter is proposed for high-power offshore wind turbines. The system uses a unidirectional-power-flow H-bridge converter as the generator-side converter, which can reduce the number of required power devices, and thus reduce the cost and improve system reliability. The proposed wind power system can work well at both the steady state and the dynamic state without increasing power losses or sacrificing control performance as evidenced by theoretical, simulation and experimental results. In addition, the low-frequency harmonics of the output voltage and current for the generator-side converter can be reduced by the presented zero deadtime modulation method. The proposed converter structure and control with minimal dc-link capacitor requirement and reduced number of active devices can be a viable solution for very large wind turbines.

REFERENCES

[1] R. M. Elavarasan, G. Shafiullah, S. Padmanaban, N. M. Kumar, A. Annam, A. M. Vetrichelvan, L. Mihet-Popa, and J. B. Holm-Nielsen, "A comprehensive review on renewable energy development, challenges, and policies of leading Indian states with an international perspective," *IEEE Access*, vol. 8, pp. 74432–74457, 2020.

[2] Global Wind Energy Condil. (2022). *Global Wind Power Report*. [Online]. Available: https://gwec.net/gwecs-global-offshore-wind-report#download

[3] J. Esch, "High-power wind energy conversion systems: State-of-the-art and emerging technologies," *Proc. IEEE*, vol. 103, no. 5, pp. 736–739, May 2015.

[4] C. Lumbreras, J. M. Guerrero, D. Fernandez, D. D. Reigosa, C. Gonzalez-Moral, and F. Briz, "Analysis and control of the inductorless boost rectifier for small-power wind-energy converters," *IEEE Trans. Ind. Appl.*, vol. 55, no. 1, pp. 689–700, Jan. 2019.

[5] Z. Zhang, Z. Li, M. P. Kazmierkowski, J. Rodríguez, and R. Kennel, "Robust predictive control of three-level NPC back-to-back power converter PMSG wind turbine systems with revised predictions," *IEEE Trans. Power Electron.*, vol. 33, no. 11, pp. 9588–9598, Nov. 2018.

[6] V. Yaramasu, B. Wu, S. Alepuz, and S. Kouro, "Predictive control for low-voltage ride-through enhancement of three-level-boost and NPC-converter-based PMSG wind turbine," *IEEE Trans. Ind. Electron.*, vol. 61, no. 12, pp. 6832–6843, Dec. 2014.

[7] T. K. A. Brekken and N. Mohan, "Control of a doubly fed induction wind generator under unbalanced grid voltage conditions," *IEEE Trans. Energy Convers.*, vol. 22, no. 1, pp. 129–135, Mar. 2007.

[8] I. Jlassi and A. J. M. Cardoso, "Fault-tolerant back-to-back converter for direct-drive PMSG wind turbines using direct torque and power control techniques," *IEEE Trans. Power Electron.*, vol. 34, no. 11, pp. 11215–11227, Nov. 2019.

[9] A. B. Abrahamsen, D. Liu, N. Magnusson, A. Thomas, Z. Azar, E. Stehouwer, B. Hendriks, G.-J. Van Zinderen, F. Deng, Z. Chen, D. Karwatzki, A. Mertens, M. Parker, S. Finney, and H. Polinder, "Comparison of levelized cost of energy of superconducting direct drive generators for a 10-MW offshore wind turbine," *IEEE Trans. Appl. Supercond.*, vol. 28, no. 4, pp. 1–5, Jun. 2018.

[10] *Siemens 14MW Wind-Turbine-SG-14-222-DD Datasheet*. Accessed: May 2020. [Online]. Available: https://www.siemensgamesa.com/en-int/products-andservices/offshore/wind-turbine-sg-14-222-dd

[11] X. Yuan, "A set of multilevel modular medium-voltage high power converters for 10-MW wind turbines," *IEEE Trans. Sustain. Energy*, vol. 5, no. 2, pp. 524–534, Apr. 2014.

[12] Z. Zhang, C. M. Hackl, and R. Kennel, "Computationally efficient DMPC for three-level NPC back-to-back converters in wind turbine systems with PMSG," *IEEE Trans. Power Electron.*, vol. 32, no. 10, pp. 8018–8034, Oct. 2017.

[13] A. Tcai, Y. Kwon, S. Pugliese, and M. Liserre, "Reduction of the circulating current among parallel NPC inverters," *IEEE Trans. Power Electron.*, vol. 36, no. 11, pp. 12504–12514, Nov. 2021.

[14] Z. Zhang, F. Wang, J. Wang, J. Rodríguez, and R. Kennel, "Nonlinear direct control for three-level NPC back-to-back converter PMSG wind turbine systems: Experimental assessment with FPGA," *IEEE Trans. Ind. Informat.*, vol. 13, no. 3, pp. 1172–1183, Jun. 2017.
[15] A. Rajaei, M. Mohamadian, and A. Y. Varjani, "Vienna-rectifier-based direct torque control of PMSG for wind energy application," *IEEE Trans. Ind. Electron.*, vol. 60, no. 7, pp. 2919–2929, Jul. 2013.
[16] A. P. Monteiro, C. B. Jacobina, F. A. D. C. Bahia, and R. P. R. De Sousa, "Vienna rectifiers for WECS applications with open-end winding PMSM," *IEEE Trans. Ind. Appl.*, vol. 58, no. 2, pp. 2268–2279, Mar. 2022.
[17] A. Satpathy, D. Kastha, and N. K. Kishore, "Vienna rectifier-fed squirrel cage induction generator based stand-alone wind energy conversion system," *IEEE Trans. Power Electron.*, vol. 36, no. 9, pp. 10186–10198, Sep. 2021.
[18] L. F. Costa, G. Buticchi, and M. Liserre, "Quad-active-bridge DC–DC converter as cross-link for medium-voltage modular inverters," *IEEE Trans. Ind. Appl.*, vol. 53, no. 2, pp. 1243–1253, Mar. 2017.
[19] Y. Zhang, X. Yuan, and M. Al-Akayshee, "A reliable medium-voltage high-power conversion system for MWs wind turbines," *IEEE Trans. Sustain. Energy*, vol. 11, no. 2, pp. 859–867, Apr. 2020.
[20] Y. Zhang, P. Zhu, X. Yuan, X. Peng, Y. Li, and X. Wu, "Low-capacitance high-power cascaded wind turbine system with instantaneous power convergence and transition," *Power Syst. Technol.*, vol. 46, no. 7, pp. 2759–2767, Jul. 2022.
[21] B. Singh, B. N. Singh, A. Chandra, K. Al-Haddad, A. Pandey, and D. P. Kothari, "A review of three-phase improved power quality AC–DC converters," *IEEE Trans. Ind. Electron.*, vol. 51, no. 3, pp. 641–660, Jun. 2004.
[22] J. Deng, H. Cheng, C. Wang, S. Wu, and M. Si, "Evaluation and comprehensive comparison of H-bridge-based bidirectional rectifier and unidirectional rectifiers," *Electronics*, vol. 9, no. 2, p. 309, Feb. 2020.
[23] S. H. Kankanala, J. W. Kimball, and A. Moeini, "Modeling and control of cascaded bridgeless multilevel rectifier under unbalanced load conditions," in *Proc. IEEE Appl. Power Electron. Conf. Expo. (APEC)*, Jun. 2021, pp. 260–266.
[24] C. Wang, Y. Zhuang, J. Jiao, H. Zhang, C. Wang, and H. Cheng, "Topologies and control strategies of cascaded bridgeless multilevel rectifiers," *IEEE J. Emerg. Sel. Topics Power Electron.*, vol. 5, no. 1, pp. 432–444, Mar. 2017.
[25] X. Yuan, "Analytical averaged loss model of a three-level T-type converter," in *Proc. 7th IET Int. Conf. Power Electron., Mach. Drives (PEMD)*, 2014, pp. 1–6.
[26] G. Liu, C. Song, and Q. Chen, "FCS-MPC-based fault-tolerant control of five-phase IPMSM for MTPA operation," *IEEE Trans. Power Electron.*, vol. 35, no. 3, pp. 2882–2894, Mar. 2020.

YONGLEI ZHANG (Member, IEEE) received the B.S. degree in electrical engineering from Henan Polytechnic University, China, in 2011, and the M.S. and Ph.D. degrees in electrical engineering from the China University of Mining and Technology, Xuzhou, China, in 2014 and 2018, respectively. Since 2021, he has been a Tenure-Track Associate Processor with the Centre for Low-Carbon Electrification Technologies and the School of Electrical Engineering, China University of Mining and Technology. His research interests include multilevel converters, wind power generation, paralleled converters, and model predictive control.

XIN PENG was born in Zaozhuang, China, in 1995. He received the B.S. degree in electrical engineering from Qingdao University, Qingdao, China, in 2019. He is currently pursuing the Ph.D. degree with the School of Electrical Engineering, China University of Mining and Technology, Xuzhou, China. His current research interests include high power wind power generation and multilevel converters.

XIBO YUAN (Senior Member, IEEE) received the B.S. degree in electrical engineering from the China University of Mining and Technology, Xuzhou, China, in 2005, and the Ph.D. degree in electrical engineering from Tsinghua University, Beijing, China, in 2010. His research interests include power electronics and motor drives, wind power generation, multilevel converters, application of wide-bandgap devices, electric vehicles, and more electric aircraft technologies.

YAN LI was born in Heze, China, in 1992. He received the M.S. degree in electrical engineering from the China University of Mining and Technology, Xuzhou, China, in 2018, where he is currently pursuing the Ph.D. degree in electrical engineering with the School of Electrical Engineering. His research interests include high power grid-connected converters and gate drive for SiC MOSFETs.

KAI WANG received the B.S. degree in electrical engineering and automation and the M.S. and Ph.D. degrees in electrical engineering from the China University of Mining and Technology, Xuzhou, China, in 2013, 2016, and 2021, respectively. Since 2021, he has been a Lecturer with the School of Electrical Engineering, China University of Mining and Technology. His current research interests include control of PWM converters, parallel converter systems, and photovoltaic generation technologies.